Journal of Biotechnology 392 (2024) 152–160

Contents lists available at ScienceDirect

Journal of Biotechnology

journal homepage: www.elsevier.com/locate/jbiotec

High-density perfusion cultures of the marine bacterium *Rhodovulum sulfidophilum* for the biomanufacturing of oligonucleotides

Francesco Iannacci [a,1], João Medeiros Garcia Alcântara [a,1], Martina Marani [a], Paolo Camesasca [a], Michele Chen [a], Fani Sousa [b], Massimo Morbidelli [a], Mattia Sponchioni [a,*]

[a] Department of Chemistry, Materials and Chemical Engineering "Giulio Natta", Politecnico di Milano, via Mancinelli 7, Milano 20131, Italy
[b] CICS-UBI – Health Sciences Research Centre, University of Beira Interior, Av. Infante D. Henrique, Covilhã 6200-506, Portugal

ARTICLE INFO

Keywords:
Perfusion
Oligonucleotides
Scale-down model
Biopharmaceuticals
Fermentation
Bench-scale bioreactor

ABSTRACT

Therapeutic oligonucleotides (ONs) are typically manufactured via solid-phase synthesis, characterized by limited scalability and huge environmental footprint, limiting their availability. Biomanufactured ONs have the potential to reduce the immunogenic side-effects, and to improve the sustainability of their chemical counterparts. *Rhodovulum sulfidophilum* was demonstrated a valuable host for the extracellular production of recombinant ONs. However, low viable cell densities and product titer were reported so far. In this work, perfusion cell cultures were established for the intensification of ON biomanufacturing. First, the perfusion conditions were simulated in 50 mL spin tubes, selected as a scale-down model of the process, with the aim of optimizing the medium composition and process parameters. This optimization stage led to an increase in the cell density by 44 % compared to the reference medium formulation. In addition, tests at increasing perfusion rates were conducted until achieving the maximum viable cell density (VCD_{max}), allowing the determination of the minimum cell-specific perfusion rate ($CSPR_{min}$) required to sustain the cell culture. Intriguingly, we discovered in this system also a maximum CSPR, above which growth inhibition starts. By leveraging this process optimization, we show for the first time the conduction of perfusion cultures of *R. sulfidophilum* in bench-scale bioreactors. This process development pipeline allowed stable cultures for more than 20 days and the continuous biomanufacturing of ONs, testifying the great potential of perfusion processes.

1. Introduction

Nucleic acids are establishing themselves as a major class of pharmaceuticals, both as therapeutics and vaccines (Yamada, 2021; Ferrazzano et al., 2023). Recent examples include the Moderna and Pfizer-BioNTech mRNA vaccines for SARS-CoV2 (Lee et al., 2023). In this scenario, oligonucleotides (ONs), short single- or double-stranded nucleic acid molecules with a number of base pairs around 20, have great potential to treat diseases due to their inhibitory or interfering functionality for post-transcriptional gene expression regulation. ONs have the ability to selectively target pre-mRNA, mRNA, or non-coding mRNA to trigger degradation, influence splicing events, or inhibit protein translation (Moumné et al., 2022; Crooke et al., 2018). Different RNA-targeted oligonucleotide classes can be identified, including antisense oligonucleotides (AONs), microRNAs (miRNAs), and short interfering RNAs (siRNAs) (Smith and Zain, 2019; Catani et al., 2020), with the first group being the most widely employed (Bajan and Hutvagner, 2020). Despite the first therapeutic oligonucleotide (fomivirsen/Vitravene) having been approved over 25 years ago (1998), only recently we have seen the number of Food and Drug Administration (FDA) and European Medicines Agency (EMA) approvals to increase (Catani et al., 2020; Egli and Manoharan, 2023a). Indeed, over these years eighteen oligonucleotides-based therapeutics have been approved for several rare and genetic diseases, such as spinal muscular atrophy, hereditary amyloidosis, and Duchenne muscular dystrophy (Xiong et al., 2021). The last approval was granted in June 2022 for the siRNA-based therapeutic vutrisiran/Amvuttra, prescribed for the treatment of hereditary transthyretin-mediated amyloidosis in adults (Egli and Manoharan, 2023b). Currently, about 100 clinical trials result as active on clinicaltrials.gov, whom 18 are actively recruiting. Though, the slow market growth reflects the limitations that are still associated to synthetic ONs. These include their poor stability in a biological environment,

* Corresponding author.
E-mail address: mattia.sponchioni@polimi.it (M. Sponchioni).
[1] The authors equally contributed.

https://doi.org/10.1016/j.jbiotec.2024.07.010
Received 2 April 2024; Received in revised form 14 June 2024; Accepted 12 July 2024
Available online 18 July 2024

immunogenicity, and inefficient manufacturing. With reference to the latter, the most established process for ON production is the solid-phase synthesis, based on the phosphoramidite chemistry (Paredes et al., 2017; Beaucage, 2008). Despite its widespread utilization, this process is affected by poor scalability, very low yield, decreasing at each added nucleotide, and by a tremendous environmental impact (Shepherd et al., 2019; Lönnberg, 2017). Factors like the employment of non-renewable reagents and starting materials, the large amount of aqueous and organic waste, the poor atom economy, and the absence of proper catalysts prevent meeting most of the 12 Green Chemistry principles (ACS Green Chemistry Institute Pharmaceutical Roundtable). Moreover, the American Chemical Society (ACS) Green Chemistry Institute Pharmaceutical Roundtable (GCIPR) estimated the process mass intensity (PMI) for the production of ONs to be in the range 3000–7000 kg of raw materials per 1 kg of product, depending upon the chain length (Andrews et al., 2021). Therefore, a more sustainable and greener alternative process must be designed for ON production.

Several studies are reporting the possibility of exploiting simple microorganisms, such as bacteria strains, to produce recombinant ONs (Ponchon and Dardel, 2007; Ponchon et al., 2009). Indeed, this approach aligns with the currently well-established industrial processes used to produce therapeutic proteins (Karst et al., 2018). In fact, the scalability of this manufacturing platform is widely recognized. In addition, it introduces the potential to decrease the environmental impact by exploiting renewable feedstocks, and the inefficiencies associated to the solid-phase synthesis. Finally, biologically produced ONs have been demonstrated to reduce the immunogenic response compared to their synthetic counterparts, thus avoiding the need for chemical modifications (Yu et al., 2019; Ho and Yu, 2016). As an example, Huang et al. (Huang et al., 2013) successfully demonstrated the possibility of exploiting *Escherichia coli* as cell host for the production of a 21-nucleotide siRNA-like molecule through plant protein p19 stabilization. However, the main limitation of this approach relies on the presence of RNases and cleavage agents in the culture medium, able to degrade the target product (Duan and Yu, 2016). To circumvent this drawback, Pereira et al. (Pereira et al., 2017, 2016) exploited a bioengineered *Rhodovulum sulfidophilum* DSM1374 strain, a gram-negative marine bacterium, reported to produce no detectable RNases. As another key property, this host is capable of recombinantly producing the human pre-miR-29b and secrete it in the extracellular medium. This avoids additional and complex steps of cell lysis and extraction steps, which are needed when ONs are produced intracellularly. Indeed, the authors reported approximately 182 μg/L and 358 μg/L of extracellular and intracellular human pre-miR-29b, respectively, after 40 hours of fermentation (Pereira et al., 2016).

Despite the favorable utilization of *R. sulfidophilum*, the few available examples of biomanufactured ONs are still extremely limited in terms of throughput, thus making this technology far from being competitive with the solid-phase synthesis. Therefore, with the aim of covering this gap and allow all the benefits of bioengineered ONs to be appreciated at large scale, an efficient upstream processing is urgently required.

In this work, we report for the first time the development of continuous perfusion cultures of *R. sulfidophilum* for the biomanufacturing of oligonucleotides. Compared to traditional batch or fed-batch fermentations, perfusion processes are amenable for higher productivity, consistent product quality, and reduced medium consumption (Wolf et al., 2019a). Moreover, they open up to the possibility of developing a continuous and integrated production system (Konstantinov and Cooney, 2015; Warikoo et al., 2012; Narayanan et al., 2022), for process intensification and reduced plant footprint (Wolf et al., 2019a).

In this direction, as schematized in Fig. 1, we first demonstrated the possibility of performing perfusion cultures of *R. sulfidophilum* in 50 mL spin tubes. In particular, the perfusion conditions were simulated by periodically spinning down the cell culture. A portion of the clarified supernatant was then removed and replaced with fresh medium, prior to resuspending the cell pellet to continue with the fermentation. We took advantage of this scale-down model and of the possibility of parallelizing multiple of these experiments to optimize the medium composition and the main process parameters (Wolf et al., 2019a, 2018). Specifically, the optimal combination of tryptone, peptone, glucose, and yeast extract was investigated with the aim of maximizing the viable cell density (VCD). Then, the role of the perfusion rate (PR) on cell growth rate and VCD was elucidated at different shaking speeds. This allowed the definition of the minimum cell-specific perfusion rate ($CSPR_{min}$), required to sustain the cell culture. In fact, this is recognized as the most convenient condition for running perfusion processes, allowing to minimize the medium consumption without inducing the destabilization of the cell culture (Wolf et al., 2019a, 2020). Intriguingly, when performing this investigation, we discovered that at medium to low shaking speeds, a $CSPR_{max}$ appears, leading to growth inhibition at higher PRs. Finally, the validation of the scale-down models was performed in a bench-scale perfusion bioreactor, integrating a 2 L stirred vessel and an alternating tangential flow filtration unit (ATF) based on hollow fiber membranes for cell retention. The study demonstrated similar $CSPR_{min}$ compared to the perfusion process simulated in spin tubes, confirming the reliability of this scale-down model.

The perfusion process developed herein confirmed the possibility of dramatically increasing the density of viable *R. sulfidophilum* cells compared to the processes reported in the literature. Additionally, the process allowed a continuous harvest of oligonucleotides, demonstrating the potential of perfusion cell cultures in favoring the widespread availability of bioengineered ONs.

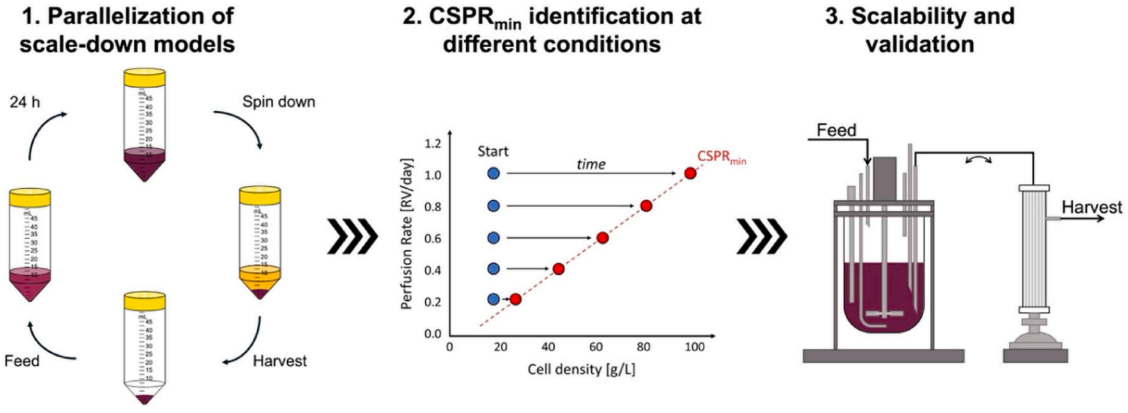

Fig. 1. Schematic procedure of up-scale perfusion process development. The leftmost panel was adapted from (Wolf et al., 2020).

2. Materials and methods

2.1. Cell line

All experiments were carried out with the marine bacterium strain *Rhodovulum sulfidophilum* DSM 1374.

2.2. Medium formulations

The nutrient medium formulations contained tryptone enzymatic digest from casein, peptone from meat, soybean meal and D-glucose (all from Millipore, USA), yeast extract, NaCl, K_2HPO_4, KH_2PO_4, $MgSO_4{\cdot}7H_2O$, $CaCl_2{\cdot}2H_2O$, $(NH_4)_2SO_4$, $FeSO_4{\cdot}7H_2O$, $MnCl_2{\cdot}4H_2O$, $CoSO_4{\cdot}7H_2O$, $CuCl_2{\cdot}2H_2O$, $ZnSO_4{\cdot}7H_2O$, H_3BO_3, $NiCl_2{\cdot}6H_2O$, $Na_2MoO_4{\cdot}H_2O$ (from Sigma-Aldrich, Germany), and HCl (Honeywell Fluka, Germany). Ultrapure biological grade water was obtained using a Milli-Q® Direct system (Millipore, USA). Cell banking and expansion were carried out using a semi-defined growth medium formulated by Pereira et al. (2016). containing 10.0 g/L tryptone, 5.0 g/L peptone, 0.5 g/L yeast extract, 513.0 mM NaCl, 23.0 mM K_2HPO_4, 7.0 mM KH_2PO_4, 278.0 mM glucose, 0.8 mM $MgSO_4{\cdot}7H_2O$, 0.3 mM $CaCl_2{\cdot}2H_2O$, 7.6 mM $(NH_4)_2SO_4$, and 1 mL of Trace Element Solution (TES). The TES was formulated as: 20.0 mM $FeSO_4{\cdot}7H_2O$, 20.0 mM $MnCl_2{\cdot}4H_2O$, 20.0 mM $CoSO_4{\cdot}7H_2O$, 2.0 mM $CuCl_2 \cdot 2H_2O$, 2.0 mM $ZnSO_4 \cdot 7H_2O$, 9.7 mM H_3BO_3, 0.2 mM $NiCl_2 \cdot 6H_2O$ and 0.2 mM $Na_2MoO_4 \cdot 2H_2O$ in 0.5 N HCl.

Regarding the composition of the media used in the optimization experiments, only the tryptone, glucose, peptone, and yeast extract concentrations were varied according to the experimental design. The concentrations of all the other nutrients were the same as in the semi-defined growth media used for cell banking and expansion.

All media solutions were sterilized either via 0.22 μm filtration (FisherBrand, USA) or in an autoclave (Systec DX65, Germany).

2.3. Expansion procedure

The initial expansion of the microbial strain was carried out in Erlenmeyer flasks, starting from a previously constructed working cell bank. On working day zero, the 1 mL vial, stored under liquid nitrogen was thawed and transferred to a 100 mL flask, to which 20 mL of reference medium had been previously added. The culture was then expanded every two days until reaching the desired volume. During this procedure the flasks were placed in an incubator (Adolf Kuhner AG, Switzerland) set at 30 °C and 80 % humidity and on an orbital shaker (Thermo Fisher Scientific, USA), set at 200 rpm.

2.4. Scale-down perfusion models

The perfusion operation was simulated in 50 mL spin tubes (TubeSpin, TPP, Switzerland), using a working volume of 10 mL and following the protocol outlined by Wolf et al. (2018, 2019b). These spin-tubes were placed in an incubator in the same conditions as mentioned previously.

On working day zero, the spin-tube was loaded with sufficient inoculum to reach the desired OD600, equal to 0.3 for the medium component screening and 5 for the perfusion parameter optimization. The daily operations were initiated with the sampling of 0.25 mL aliquots from the spin-tube and analysis for OD600, ammonia, and glucose concentration (see Section 2.7). In order to simulate the PR, after centrifugation (Thermo Fisher SL16, USA) at 18,500 rcf for 8 min, a certain volume of the supernatant was discarded and replaced with fresh medium to cover the range 0.05 – 1 reactor volumes (RV)/day and the pellet resuspended. The supernatant was then frozen at −80 °C for further analysis.

2.5. Bench-scale bioreactor operation

The scale-up was performed in a 2 L stirred tank vessel (Vaudaux-Eppendorf, Switzerland) connected to an alternating tangential flow filtration (ATF) unit as cell-retention device to ensure the perfusion operation. The unit comprises a hollow-fiber membrane (0.5 μm, PES, 1570 cm^2, Repligen, USA) and a diaphragm pump, including controller (Repligen, USA). The experimental runs were performed at 30 °C, pH 7, Dissolved Oxygen (DO) 20 % v/v and stirring speed at 500 rpm, which were kept constant throughout the trials. The monitoring and control of the bioreactor were conducted using the DASGIP Control software (Eppendorf, Germany). Temperature control was ensured using a heating mantel and pH regulation via addition of pH buffers and carbon dioxide. DO concentration was adjusted by acting on the oxygen flowrate. The mixing in the bioreactor was ensured by a Rushton impeller installed at the bottom of the transmission shaft. The inlet gaseous stream was filtered through an air filter (Midisart 2000, 0.22 μm, PTFE, Sartorius, Germany) and inserted directly in the culture vessel via a 7-hole sparger. Based on measured DO value, the oxygen inlet concentration varied between 21 % and 40 % and the total inlet flowrate was in the range 30–50 sL/h. To prevent foam formation, 5 % v/v Antifoam B emulsion (Sigma-Aldrich, USA) was added manually while a Marine impeller was mounted above the liquid level. The bioreactor and related inlet and outlet bottles were kept on scales (Mettler Toledo, USA) to monitor the actual flowrates.

2.6. Extracellular RNA extraction

The extracellular nucleic acids produced by *R. sulfidophilum* were recovered from the supernatant of the samples and from the harvest stream of the reactor by precipitation with ethanol, based on the protocol developed by Pereira et al. (2016). The cell-free supernatant, generally taken in 1 mL amounts, was mixed with 0.1 volumes of 0.1 M sodium acetate (Sigma-Aldrich, USA), 3 volumes of ice-cold 99.9 % ethanol (Sigma-Aldrich, USA) and vortexed. The sample was then incubated for two hours at −80 °C, centrifuged at maximum speed (4500 g) at 4 °C for 30 min and the resulting pellet was washed twice with 0.5 mL of ice-cold 75 % ethanol, with further centrifugation at 4 °C for 10 min after each wash. After the removal of the ethanol, the pellet was dried with a flow of compressed air and then resuspended in Milli-Q water to reach the initial volume.

2.7. Analytics

Measurements of the optical density at 583 nm, as indication of the cell density, were performed with a Cedex Bio analyzer (Roche Diagnostics AG, Basel, Switzerland).

Glucose concentration was determined via high performance liquid chromatography (HPLC) (Agilent Technologies 1200, Germany). The analytical method exploited an isocratic elution at 0.3 mL/min of 14 mM H_2SO_4 on an Aminex HPX-87 H Ion Exclusion Column (Bio-Rad, USA) at 50 °C. UV detection was carried with a diode array detector set at 190 nm (Jalaludin and Kim, 2021).

ON quantification was performed by measuring the absorbance at 260 nm with baseline normalization at 340 nm in a UV-Vis spectrophotometer Jasco V-630 (Jasco Europe s.r.l., Italy). The extinction coefficient used for content evaluation was the average value for single-stranded RNA, equal to 40 ng/μL. From here, a HPLC analytical method was defined, calibrated based on spectrophotometer measurements and further employed. The method used an Ion-Pair Reversed-Phase (IP-RP) AdvanceBio Oligonucleotides column 2.1 ×100 mm (Agilent Technologies, Germany) at 50 °C with the UV detector set at 260 nm. The aqueous mobile phase was 100 mM hexafluoro-2-propanol (HFIP) and 4 mM triethylamine (TEA) in H_2O and the elution phase was a 50 % v/v methanol/water (MeOH/H_2O) solution (Biba et al., 2017; Apffel et al., 1997). A gradient from 0 % to 100 % of organic phase in

10 min was used to desorb oligonucleotides from the stationary phase.

2.8. Statistical analysis

The results are reported as mean value ± standard deviation if not otherwise stated. For the medium optimization, statistical analysis was performed through one-way analysis of variance setting a threshold of 0.05 and using Tukey's test for means comparison.

3. Results and discussion

3.1. Perfusion medium optimization

The optimization of the nutrient composition represents the first step in the direction of an intensification in ON biomanufacturing. Since it has been previously shown (Karst et al., 2018) that the medium developed for batch and fed-batch processes does not necessarily translate into the best for perfusion cultures, this optimization was carried out in 50 mL spin tubes operated to simulate the perfusion process, being a proven scale-down model for this type of operation (Wolf et al., 2018). Therefore, we performed a series of experiments to decouple and investigate the effect of each nutrient, testing the different sources individually. A preliminary screening was performed for the carbon source, *i.e.* glucose, as reported in Figure S1. The analysis was carried out in batch scale-down models based on the medium composition defined by Pereira et al. (Pereira et al., 2016). Hence, the exploration range was defined by three levels of glucose concentration, namely 7 g/L (-30 % pre-defined concentration), 10 g/L (pre-defined concentration), 13 g/L (+30 % pre-defined concentration). The influence of glucose concentration is highly impacting on cellular growth. Indeed, higher glucose amount performed better with respect to the pre-defined carbon source concentration. Therefore, we started from this investigation and analyzed higher concentrations, in the range 13–50 g/L (see Fig. 2A), in 50 mL spin tubes simulating perfusion conditions. In this set of experiments, the concentration of the nitrogen sources (*i.e.* tryptone, peptone and yeast extract) was as defined in the reference medium (see Section 2.2). Regarding the nitrogen sources instead, their effect was studied individually. Peptone, yeast extract and tryptone are all complex nitrogen sources. Therefore, it is possible to increase the concentration of the same peptide when mixing these nutrients. Hence, in order to compare them in similar nitrogen supply conditions, their individual nitrogen content was evaluated from their certificate of analysis. In this way, concentrations in the range 9.5–37.9 g/L, 10.0–40.0 g/L, and 11.2–44.7 g/L were considered for peptone, tryptone and yeast extract, respectively (see Fig. 2B, C, D).

With reference to Fig. 2A, we observed a monotonic increase in the cell density with time at each tested glucose concentration. However, by comparing the VCD at 96 h (red bars), only non-significant changes were observed across the tested concentrations. Hence, since an increase in the glucose concentration and, in turn, of the medium cost is not justified, we decided to fix it to the intermediate level of 30 g/L for all the subsequent experiments. In the case of the nitrogen sources, the VCD increased proportionally to the peptone concentration in the whole range investigated, as shown in Fig. 2B. On the other side, a maximum cell density was observed for both tryptone (Fig. 2C) and yeast extract (Fig. 2D). This was reached at 30 g/L of tryptone and 22.4 g/L for the yeast extract. Above these thresholds, inhibitory conditions were reached, leading to a reduced cell proliferation rate. Considering the VCD reached at 96 h (red bars) for the three nitrogen sources, the most promising results were achieved using peptone and yeast extract, leading to a maximum value of 4.14 and 4.11 g/L, respectively. Hence, since the VCD for peptone could still be increased, higher concentrations were

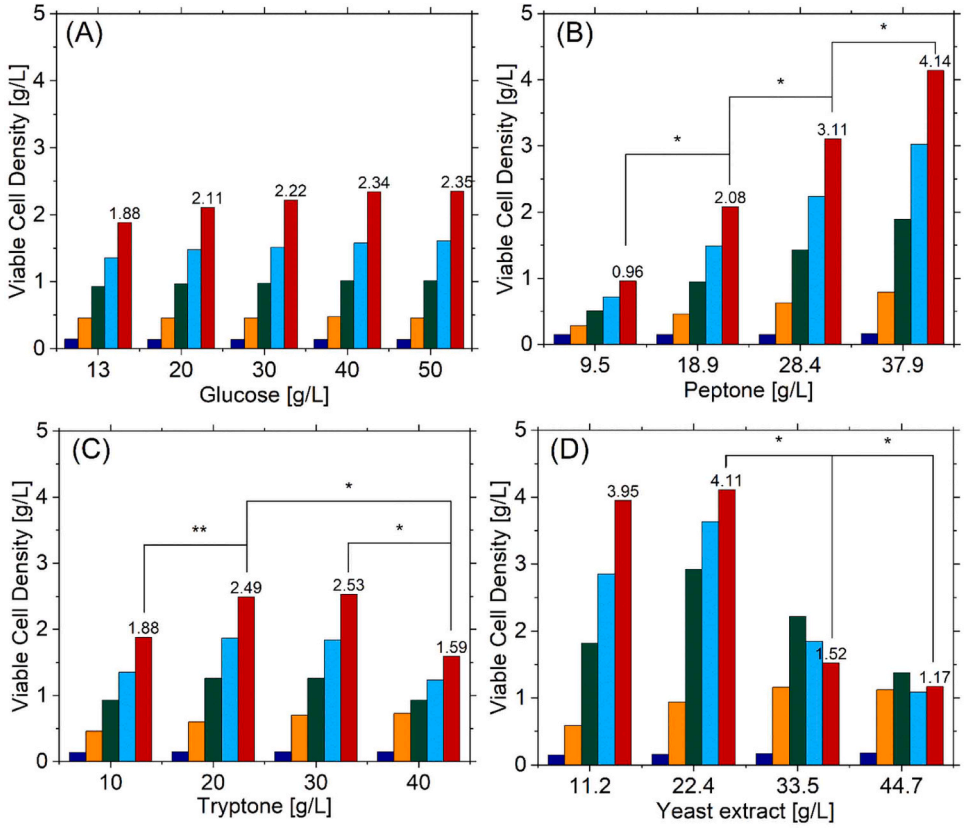

Fig. 2. VCD during operation time for perfusion experiments simulated in 50 mL spin tubes at different concentrations of individual nutrients: glucose (A), peptone (B), tryptone (C), and yeast extract (D). 0 h = blue bars, 24 h = orange bars, 48 h = green bars, 72 h = light blue bars, 96 h = red bars. Statistical analysis was performed only for the data taken at 96 h (red bars) using one-way ANOVA: *$p<0.05$, **$p<0.15$.

tested until a maximum of 55 g/L, while in the case of yeast extract a refinement in proximity of the concentration leading to the maximum cell density was studied, performing experiments from 13 to 23 g/L. The results of these experiments are shown in Table 1.

While tryptone yielded the worst results, with a decrease in the VCD by 7.6 % with respect to the reference formulation, both peptone and yeast extract could outperform the reference medium, with a maximum gain in VCD of 72 % and 50 %, respectively. The factors considered in the choice of the nitrogen source were then the concentration and the cost per liter of medium. Even though the VCD reached with peptone was slightly higher compared to yeast extract, this gain came at higher concentration of the nitrogen source (increasing the osmolality of the medium) and consequently at higher cost, also given that peptone is more expensive than yeast extract. Therefore, yeast extract was selected for further experiments, with a concentration between 11 and 23 g/L. These were performed by increasing the OD for the inoculum from 0.3 to 5. As confirmed in Table 1, in this way we could conclude the optimal concentration of this nitrogen source to be in the range 13 – 15 g/L, leading to a VCD of 6.8 g/L. Therefore, the selected yeast extract concentration for further experiments was set to 13 g/L.

Overall, the preliminary optimization performed on the carbon and nitrogen sources led to an optimal glucose concentration of 30 g/L and to the selection of yeast extract as the most performing nitrogen source, used with a concentration of 13 g/L. This formulation tested in a simulated perfusion cell culture allowed to increase the VCD by 50 % with respect to the reference medium, with evident benefits in terms of ON productivity.

3.2. Design space for the perfusion cultures of R. sulfidophilum

Based on the optimal medium formulation, the next step for developing a successful perfusion process is to define its design space, in terms of VCD and PR. This space is inferiorly limited by the minimum cell-specific PR ($CSPR_{min}$), defined for a certain medium formulation as the minimum PR required to sustain a given VCD. In general, it was demonstrated that, in a perfusion cell culture, it is desirable to work at the $CSPR_{min}$ in order to maximize the productivity while minimizing the medium consumption. As proposed by Konstantinov et al. (2006) and Wolf et al. (2018), two methods can be adopted to identify this optimal condition: the "push-to-low" approach, where the CSPR is progressively decreased by decreasing PR at constant VCD, and the "push-to-high" approach, where the VCD is increased in steps with a constant PR.

To define the $CSPR_{min}$, here we adopted the push-to-high approach. Due to the intrinsically discontinuous scale-down process used in this work, only PR $\leq$ 1 RV/day could be tested. On the other side, with this scale-down model, several experiments could be run in parallel, exploring PR between 0.05 and 1 RV/day with reduced waste of raw materials. The different perfusion experiments were run until the maximum VCD (VCD_{max}) at the considered PR was achieved, representing the maximum number of viable cells that specific PR can sustain. Since in this simplistic bioreactor the oxygen is supplied to the culture in a passive way, through the area exposed to the atmosphere, we hypothesized that the limited oxygen transfer rate (OTR) may introduce cell growth limitations (Zhang et al., 2009). For this reason, the analysis of the perfusion design space was performed at different speeds of the orbital shaker, specifically at 200, 260, and 320 rpm, which directly act on the contact area at the air/liquid interface. The evolution of the VCD during time for each combination of PR and shaking speed is shown in Figure S2-S4 (see Supporting Information Section).

The VCD reached at steady-state is then reported for each experiment as a function of PR in Fig. 3.

Here, it is possible to observe a good consistency in the maximum VCD reached at PRs 0.05–0.4 RV/day across all the shaking speeds. This lower limitation is fully described in the literature and corresponds to the mentioned $CSPR_{min}$. This limitation is normally linear, meaning the higher the PR, the higher the maximum cell density achievable in the reactor. In these experiments, this trend is indeed valid for the largest shaking speed (*i.e.* 320 rpm) and, to a certain extent, at 260 rpm.

On the other hand, for the experiments conducted at 200 rpm, this linear trend was observed only for low PR in the range 0.05–0.3 RV/day. For higher values, an upper and opposite limitation appears. Intriguingly, it appears that additional medium supplied to the culture corresponds to lower viable cell densities at steady state. We defined this unexpected growth limitation as $CSPR_{max}$, to establish a symmetry with the concept of $CSPR_{min}$ widely reported in the literature. Several factors could be contributing to the presence of a $CSPR_{max}$. For example, medium inhibition could be a cause, since it has been documented (see Fig. 2D) that too high concentrations of yeast extract could lead to growth inhibition and hence to lower VCD. However, if this were the sole factor, it should also occur for higher shaking speeds. Since this is not the case, it is evident that limitations associated with oxygen supply are involved, as demonstrated by the fact that this $CSPR_{max}$ disappears as we move to higher shaking speeds, such as 320 rpm, which corresponds to higher OTR. Still, this behavior had not yet been observed when using spin tubes as scale-down models, since most of the cell lines employed for perfusion operations are mammalian, which have lower oxygen uptake rates than typical bacterial cell lines (Huang and McDonald, 2009).

From these results, it is possible to calculate the $CSPR_{min}$ and, when present, the $CSPR_{max}$ for each of the shaking speeds (see Table S1-S2). With this information, the PR can be chosen for a desired VCD in the

Table 1
VCD measured in scale-down perfusion experiments after 96 h from inoculum for different nitrogen source concentrations and comparison with reference medium. For all the experiments, the glucose concentration was fixed to 13 g/L.

Medium Type	Nitrogen Source [g/L]			Viable Cell Density [g/L]	
	Tryptone	Peptone	Yeast Extract	Inoc. OD 0.3	Inoc. OD 5
Reference Medium	10	5	0.5	2.73	
Tryptone	30			2.52	
Peptone		38		4.14	
		45		4.52	
		50		4.64	
		55		4.70	
Yeast Extract			11	3.95	6.69
			13		6.77
			15		6.79
			19		5.10
			22	4.10	
			23		3.70

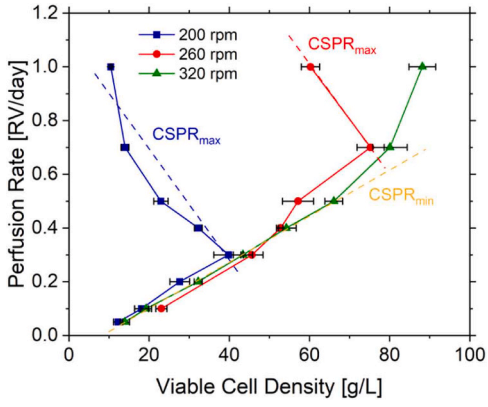

Fig. 3. PR vs VCD for the scale-down push-to-high experiments at 200, 260, and 320 rpm as shaking speeds. Data points correspond to mean values of VCD at stationary growth phase. Error bars represent standard deviation.

region defined by the $CSPR_{min}$ and $CSPR_{max}$ with the confidence that it will not limit cellular growth. In this design space, as already discussed, the optimal condition is defined by the $CSPR_{min}$ itself, allowing to maximize productivity while minimizing the medium consumption. It is worth mentioning that these values correspond to the minimum medium amount that needs to be supplied in order to sustain the desired cell culture without inducing cellular destabilization. However, it has been previously observed that $CSPR_{min}$ values determined in VCD_{max} experiments may not be able to sustain long-term perfusion cultures (Wolf et al., 2019b). Therefore, these $CSPR_{min}$ can also be interpreted as $CSPR_{crit}$, which corresponds to the critical quantity of medium necessary to be supplied. However, in the experiments conducted by Bielser et al. (Bielser et al., 2018), the determination of the $CSPR_{min}$ via this method in spin tubes and deep-well plates was found to allow long-term perfusion runs in benchtop bioreactors. Nevertheless, in the experiments reported, the bacteria strain used has shown prolonged stability over time, hence we consider the obtained values as the $CSPR_{min}$. Moreover, it should be pointed out that the values determined correspond only to the specific medium composition used. In fact, a more concentrated medium and hence higher medium depth (Wolf et al., 2020; Medeiros Garcia Alcântara and Sponchioni, 2022) would decrease the $CSPR_{min}$. Yet, this can also lead to added complication of higher osmolality in the cell culture, which can inhibit microbial growth (Konstantinov et al., 2006).

3.3. Bench-scale perfusion process

After having defined the optimal perfusion conditions in scale-down models, we scaled up the operation to a working volume of 2 L in a stirred tank bioreactor equipped with an ATF for continuous cell retention. This represents the first report on the biomanufacturing of ONs through a perfusion process. In particular, perfusion cultures of *R. sulfidophilum* were investigated at different PR, namely 0.5, 0.7, and 1 RV/day, with the aim of highlighting its impact on the main process variables, such as the maximum VCD, nutrient consumption, and ON titer. These parameters were tracked during the operation time and reported in Fig. 4 for PR = 0.5 RV/day and in Figure S5 for PR = 0.7 and 1 RV/day.

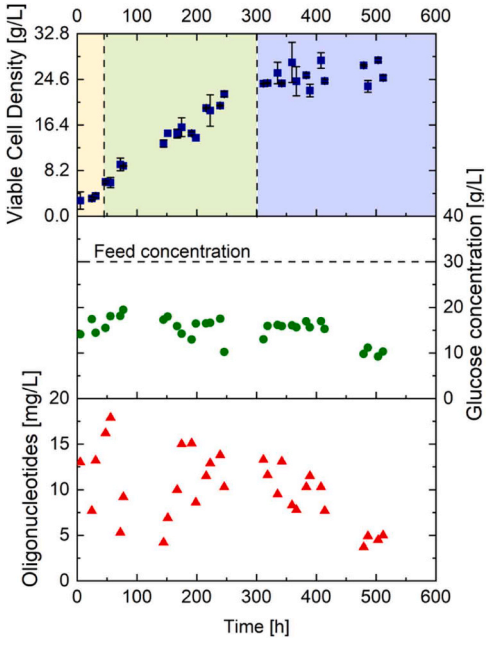

Fig. 4. VCD, glucose, and oligonucleotide concentration during time for the perfusion experiment conducted at 0.5 RV/day in the bench-scale bioreactor. Yellow = lag phase, green = exponential phase, blue = stationary phase. In VCD graph, data points represent mean values. Error bars correspond to standard deviation calculated from at least three values.

First, it is possible to appreciate the stability of the process, which could be run for more than 20 days at each PR in this scaled-up configuration. By looking at the trend of the VCD during time, the three characteristic phases of cell growth, including the lag, exponential, and stationary ones, can be distinguished, with the latter starting approximately at 300 h. In this condition, the VCD reached an average value of 27 g/L, which corresponds to an OD of 50 StdU and therefore to a 10-fold OD increase with respect to reference results (Pereira et al., 2016). Glucose, as carbon source, was continuously fed to the system at 30 g/L and its concentration in the bioreactor reached very soon a steady-state value of 15 g/L, as a result of cell uptake. The concentration of produced ON was also tracked during the operation time via HPLC. This confirmed the possibility of obtaining a continuous extracellular harvest of nucleic acids with the perfusion process. Interestingly, after a scattered trend during the initial period, a monotonic decrease was observed. We then hypothesized that the production of extracellular nucleic acids is mainly obtained during cellular growth, as it happens for primary metabolites. Since the former was mainly observed during the lag and growth phases, it seems that ONs do not originate from cell autolysis but rather result from ongoing active expression, similarly to results reported in the literature (Ando et al., 2006). This confirmed the possibility of biomanufacturing ONs using perfusion processes, which are known to dramatically increase the productivity compared to their discontinuous or semi-continuous counterparts (Yang et al., 2000; Bielser et al., 2019; Gagnon et al., 2018). This appealing solution can be then envisioned to improve the sustainability and alleviate the scalability concerns currently associated with ON manufacturing via solid-phase synthesis.

In order to assess the scalability of the results obtained in our scale-down model, the two different perfusion processes, simulated in spin tubes shaken at 320 rpm and performed in the bench-scale bioreactor, are compared in Fig. 5A in terms of VCD reached at steady-state for each tested PR. The evolution of this parameter during time is reported for the different experiments in the bioreactor in Figure S6 and Figure S7.

The expected monotonic increase of VCD with PR (see Fig. 5 A) is maintained also for bench-scale operations, obtaining 27, 50, and 70 g/L of maximum VCD for 0.5, 0.7, and 1 RV/day, respectively. This confirmed the existence, for both systems, of a $CSPR_{min}$, represented by the dashed lines. This shows the same intercept with the x-axis for both the micro- and bench-scale, which refers to a situation where no medium is provided during time, and hence to a batch process. Moreover, the liter-scale tests revealed the absence of a $CSPR_{max}$, indicating no medium limitation at high PR. This confirmed that oxygen transfer limitations may have been the responsible for this inhibition at low shaking speeds in the spin tubes. Comparing again the two different scales, it can be observed a considerable shift towards lower VCD at the same PR for the bench-scale bioreactor. In other words, the bioreactor required a higher PR to sustain the same VCD as the scale-down model. A possible reason might be due to the utilization of Rushton impellers mounted on the transmission shaft. Indeed, although these devices are crucial for proper mixing and dissolution of oxygen in the liquid broth, cells can experience damage due to the presence of high shear stress located close to the mechanical devices (Nienow, 2021; Pörtner, 2015; Buffo et al., 2016). Nevertheless, another concern may arise from bubble formation and related shear and normal stresses. Again, air sparger is crucial for having an active oxygen supply, conversely to the passive transfer occurring in micro-scale models, especially for bacteria cultivations since their oxygen uptake rate is typically higher than for mammalian cells (He et al., 2019). Despite the presence of a cellular wall in bacteria, which guarantees a better resistance to bubble-associated shears (Chisti, 2000; Esperança et al., 2020), it is possible that a fraction of viable cells undergoes high stresses, particularly on the liquid surface where bubbles burst. At last, it should also be considered that, contrarily to small-scale models, higher working volumes negatively impact the nutrient transport inside the broth itself (Koynov et al., 2007).

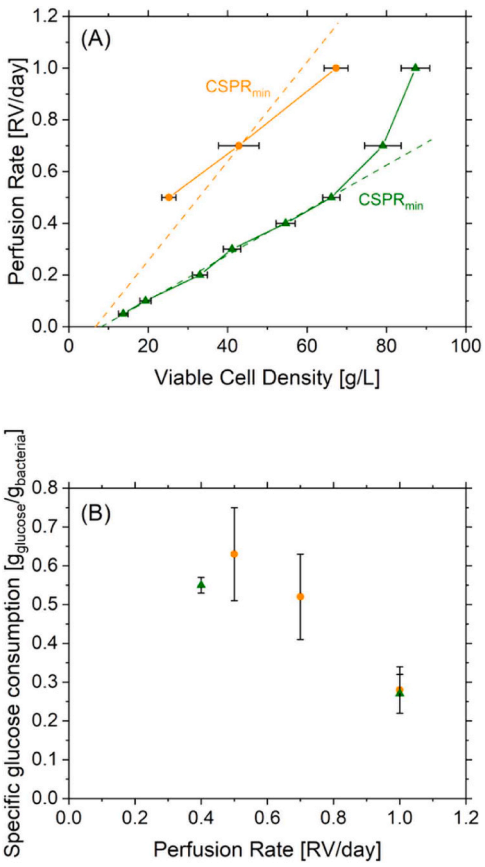

Fig. 5. (A) Comparison of $CSPR_{min}$ at bench-scale (orange circles) and 320 rpm micro-scale (green triangles) perfusion systems. (B) Comparison of specific glucose consumption for bench- (orange circles) and micro-scale at 320 rpm (green triangles) at steady state. In both graphs, data points represent the mean values of VCD (A) and specific glucose consumption (B) at stationary growth phase. Error bars correspond to standard deviation measured from at least three valuees.

Not only cellular growth, but also the influence of PR on carbon source consumption was investigated. In Fig. 5B, the cell-specific glucose consumption is reported as a function of PR for both the liter- and micro-scale systems. The graph refers to the steady-state values of glucose and cellular concentration. Hence, once the microorganisms have reached this phase, achieving the largest possible population, the glucose concentration reaches a constant value which is independent of PR, as demonstrated in Figure S7. Since, instead, the VCD icreases with PR, this situation is reflected in a lower specific nutrient consumption for higher PR. Indeed, both systems show a similar behavior with a monotonic decrease at increasing PR and a very similar cell-specific glucose consumption in both spin tubes and perfusion bioreactor.

At last, the influence of PR on oligonucleotides production was evaluated. The great advantage of perfusion systems is the continuous recovery of extracellular products, like ONs in this case, in the clarified harvest. In addition, this operation allows working at steady-state, where product titer and quality are consistently preserved (Walther et al., 2019; Meuwly et al., 2004). This is important to ensure high safety for biotherapeutics. For this reason, in Fig. 6 we reported the average ON concentration after the steady-state in VCD was reached (approximately after 300 h).

From Fig. 6, it is evident that the ON concentration in the harvest monotonically increases with PR, reaching average stationary concentrations of 8.7, 9.2, and 11.5 mg/L at PR = 0.5, 0.7, and 1 RV/day, respectively. Therefore, the increasing cellular population at higher PR significantly enhances the overall product expression.

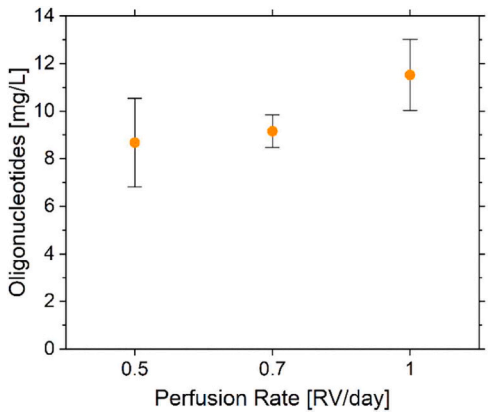

Fig. 6. Stationary oligonucleotides concentration at different PRs for bench-scale operations. Points represent the mean values of oligonucleotides concentrations at stationary growth phase, error bars represent the standard deviation of at least three data points.

Overall, the maximum oligonucleotide concentration of 11.5 mg/L we reached was in the 2 L scale bioreactor with a PR of 1 RV/day. Despite this product titer is much lower than the one commonly reported for monoclonal antibodies, it is worth highlighting: (i) the significantly lower dosage required for ONs (*e.g.* 12 mg for Spinraza (nusinersen), 21 mg for Onpattro (patisiran) for 70 kg body weight); (ii) to the best of our knowledge this is the highest concentration in the oligonucleotide production reported from fermentation processes (Catani et al., 2020). Indeed, in the work of Pereira et al. (Pereira et al., 2016), the authors reported an ON titer of 0.182 mg/L in a fed-batch cell culture. Hence, the developed perfusion process showed the potential to greatly improve titers when compared to discontinuous processes, thus testifying the possibility of significantly boosting the productivity of biomanufactured ONs.

4. Conclusions

Oligonucleotide-based pharmaceuticals are evermore getting significance and correspondingly being produced in large amounts, boosted by the advent of mRNA-based vaccines for SARS-CoV2. Although currently these drugs are mostly produced via solid-phase synthesis, fermentation processes carry the potential for cost reduction and circumvention of possible immunogenic effects but are still far from being competitive in terms of productivity. Here, as it was the case for the production of therapeutic proteins (Karst et al., 2018), perfusion cell cultures can lead to a decisive breakthrough, surpassing their fed-batch counterparts in terms of productivity and product consistency. In this work, the conversion of a batch process for the production of oligonucleotides to perfusion was investigated, starting from the optimization of the medium composition and the definition of the process design space operated in 50 mL spin tubes as scale-down models. The medium optimization was performed to investigate the effect of the single carbon and nitrogen sources provided to the cell culture, obtaining a higher understanding in perfusion scale-down models. This optimization led to an increase in optical density of 44 % with respect to the reference medium formulation. After this optimization, a series of VCD_{max} experiments were carried out in order to highlight the perfusion design space (Wolf et al., 2020; Medeiros Garcia Alcântara and Sponchioni, 2022). These trials were performed at different shaking speeds, thus at different oxygen transfer rates. Based on these experiments, the $CSPR_{min}$ was determined. Furthermore, the concept of $CSPR_{max}$ was introduced, above which the cell culture will suffer growth inhibition. The analysis of the optimal perfusion conditions was then leveraged to realize the first example of perfusion cultures of *R. sulfidophilum* for the biomanufacturing of oligonucleotides at a bench-scale. Here, the influence

of PR on cell growth, nutrient consumption, and ONs production was examined. From these bioreactor runs, the oligonucleotide titer could be significantly increased when compared to a previous work (Pereira et al., 2016) with the same strain. This testifies the promises hold by perfusion cultures of *R. sulfidophilum* for the large-scale bio-manufacturing of ONs, which could eventually compete with those synthesized via solid-phase synthesis, allowing to appreciate the above-mentioned advantages of biologically-expressed oligonucleotides.

It is worth mentioning that the process shown here is not exempted from the production of impurities, which could be either associated to the specific process used for expression (*e.g.* cell debris, host cell proteins and DNA) or variants of the main product. For this reason, as in all biotech processes, a suitable downstream processing needs to be designed to remove such impurities before distribution of the active principle. Still, this can leverage the experience established on other recombinant biotherapeutics, like monoclonal antibodies.

CRediT authorship contribution statement

Francesco Iannacci: Writing – original draft, Investigation, Data curation. **Mattia Sponchioni:** Writing – review & editing, Supervision, Project administration. **Massimo Morbidelli:** Writing – review & editing, Supervision. **Fani Sousa:** Writing – review & editing, Resources. **Michele Chen:** Validation, Investigation. **Paolo Camesasca:** Validation, Investigation. **Martina Marani:** Validation, Investigation. **João Medeiros Garcia Alcântara:** Writing – review & editing, Investigation, Data curation.

Declaration of Competing Interest

The authors declare that they have no known competing financial interests or personal relationships that could have appeared to influence the work reported in this paper.

Data availability

Data will be made available on request.

Appendix A. Supporting information

Supplementary data associated with this article can be found in the online version at doi:10.1016/j.jbiotec.2024.07.010.

References

ACS Green Chemistry Institute Pharmaceutical RoundtableTools for Innovation in Chemistry", [Online]. Available: ⟨https://www.acsgcipr.org/tools-for-innovation-in-chemistry/⟩.

Ando, T., Suzuki, H., Nishimura, S., Tanaka, T., Hiraishi, A., Kikuchi, Y., 2006. Characterization of extracellular RNAs produced by the marine photosynthetic bacterium Rhodovulum sulfidophilum. J. Biochem. 139 (4), 805–811. https://doi.org/10.1093/jb/mvj091.

Andrews, B.I., et al., 2021. Sustainability challenges and opportunities in oligonucleotide manufacturing. J. Org. Chem. 86 (1), 49–61. https://doi.org/10.1021/acs.joc.0c02291.

Apffel, A., Chakel, J.A., Fischer, S., Lichtenwalter, K., Hancock, W.S., 1997. Analysis of oligonucleotides by HPLC–electrospray ionization mass spectrometry. Anal. Chem. 69 (7), 1320–1325. https://doi.org/10.1021/ac960916h.

Bajan, S., Hutvagner, G., 2020. RNA-based therapeutics: from antisense oligonucleotides to miRNAs. Cells 9 (1), 137. https://doi.org/10.3390/cells9010137.

Beaucage, S.L., 2008. Solid-phase synthesis of siRNA oligonucleotides. Curr. Opin. Drug Discov. Dev. 11 (2), 203–216. ⟨http://www.ncbi.nlm.nih.gov/pubmed/18283608⟩ ([Online]. Available:).

Biba, M., Foley, J.P., Welch, C.J., 2017. Liquid chromatographic separation of oligonucleotides. In: Liquid Chromatography. Elsevier, pp. 159–182. https://doi.org/10.1016/B978-0-12-805392-8.00006-2.

Bielser, J.-M., Chappuis, L., Xiao, Y., Souquet, J., Broly, H., Morbidelli, M., 2019. Perfusion cell culture for the production of conjugated recombinant fusion proteins reduces clipping and quality heterogeneity compared to batch-mode processes. J. Biotechnol. 302, 26–31. https://doi.org/10.1016/j.jbiotec.2019.06.006.

Bielser, J.-M., Wolf, M., Souquet, J., Broly, H., Morbidelli, M., 2018. Perfusion mammalian cell culture for recombinant protein manufacturing – a critical review. Biotechnol. Adv. 36 (4), 1328–1340. https://doi.org/10.1016/j.biotechadv.2018.04.011.

Buffo, M.M., Corrêa, L.J., Esperança, M.N., Cruz, A.J.G., Farinas, C.S., Badino, A.C., 2016. Influence of dual-impeller type and configuration on oxygen transfer, power consumption, and shear rate in a stirred tank bioreactor. Biochem Eng. J. 114, 130–139. https://doi.org/10.1016/j.bej.2016.07.003.

Catani, M., et al., 2020. Oligonucleotides: current trends and innovative applications in the synthesis, characterization, and purification. Biotechnol. J. 15 (8) https://doi.org/10.1002/biot.201900226.

Chisti, Y., 2000. Animal-cell damage in sparged bioreactors. Trends Biotechnol. 18 (10), 420–432. https://doi.org/10.1016/S0167-7799(00)01474-8.

Crooke, S.T., Witztum, J.L., Bennett, C.F., Baker, B.F., 2018. RNA-Targeted Therapeutics. Cell Metab. 27 (4), 714–739. https://doi.org/10.1016/j.cmet.2018.03.004.

Duan, Z., Yu, A.-M., 2016. Bioengineered non-coding RNA agent (BERA) in action. Bioengineered 7 (6), 411–417. https://doi.org/10.1080/21655979.2016.1207011.

Egli, M., Manoharan, M., 2023a. Chemistry, structure and function of approved oligonucleotide therapeutics. Nucleic Acids Res. 51 (6), 2529–2573. https://doi.org/10.1093/nar/gkad067.

Egli, M., Manoharan, M., 2023b. Chemistry, structure and function of approved oligonucleotide therapeutics. Nucleic Acids Res. 51 (6), 2529–2573. https://doi.org/10.1093/nar/gkad067.

Esperança, M.N., Mendes, C.E., Rodriguez, G.Y., Cerri, M.O., Béttega, R., Badino, A.C., 2020. Sparger design as key parameter to define shear conditions in pneumatic bioreactors. Biochem Eng. J. 157, 107529 https://doi.org/10.1016/j.bej.2020.107529.

Ferrazzano, L., Corbisiero, D., Tolomelli, A., Cabri, W., 2023. From green innovations in oligopeptide to oligonucleotide sustainable synthesis: differences and synergies in TIDES chemistry. Green. Chem. 25 (4), 1217–1236. https://doi.org/10.1039/D2GC04547H.

Gagnon, M., Nagre, S., Wang, W., Hiller, G.W., 2018. Shift to high-intensity, low-volume perfusion cell culture enabling a continuous, integrated bioprocess. Biotechnol. Prog. 34 (6), 1472–1481. https://doi.org/10.1002/btpr.2723.

He, C., Ye, P., Wang, H., Liu, X., Li, F., 2019. A systematic mass-transfer modeling approach for mammalian cell culture bioreactor scale-up. Biochem Eng. J. 141, 173–181. https://doi.org/10.1016/j.bej.2018.09.019.

Ho, P.Y., Yu, A., 2016. Bioengineering of noncoding RNAs for research agents and therapeutics. WIREs RNA 7 (2), 186–197. https://doi.org/10.1002/wrna.1324.

Huang, L., Jin, J., Deighan, P., Kiner, E., McReynolds, L., Lieberman, J., 2013. Efficient and specific gene knockdown by small interfering RNAs produced in bacteria. Nat. Biotechnol. 31 (4), 350–356. https://doi.org/10.1038/nbt.2537.

Huang, T.-K., McDonald, K.A., 2009. Bioreactor engineering for recombinant protein production in plant cell suspension cultures. Biochem Eng. J. 45 (3), 168–184. https://doi.org/10.1016/j.bej.2009.02.008.

Jalaludin, I., Kim, J., 2021. Comparison of ultraviolet and refractive index detections in the HPLC analysis of sugars. Food Chem. 365, 130514 https://doi.org/10.1016/j.foodchem.2021.130514.

Karst, D.J., Steinebach, F., Morbidelli, M., 2018. Continuous integrated manufacturing of therapeutic proteins. Curr. Opin. Biotechnol. 53, 76–84. https://doi.org/10.1016/j.copbio.2017.12.015.

K. Konstantinov *et al.*, The 'Push-to-Low' Approach for Optimization of High-Density Perfusion Cultures of Animal Cells, 2006, pp. 75–98. doi: ⟨10.1007/10_016⟩.

Konstantinov, K.B., Cooney, C.L., Mar. 2015. White paper on continuous bioprocessing May 20–21 2014 continuous manufacturing symposium. J. Pharm. Sci. 104 (3), 813–820. https://doi.org/10.1002/jps.24268.

Koynov, A., Tryggvason, G., Khinast, J.G., 2007. Characterization of the localized hydrodynamic shear forces and dissolved oxygen distribution in sparged bioreactors. Biotechnol. Bioeng. 97 (2), 317–331. https://doi.org/10.1002/bit.21281.

Lee, K.-M., Lin, S.-J., Wu, C.-J., Kuo, R.-L., Feb. 2023. Race with virus evolution: The development and application of mRNA vaccines against SARS-CoV-2. Biomed. J. 46 (1), 70–80. https://doi.org/10.1016/j.bj.2023.01.002.

Lönnberg, H., 2017. Synthesis of oligonucleotides on a soluble support. Beilstein J. Org. Chem. 13, 1368–1387. https://doi.org/10.3762/bjoc.13.134.

J. Medeiros Garcia Alcântara and M. Sponchioni, Evolution and design of continuous bioreactors for the production of biological products, 2022, pp. 1–26. doi: ⟨10.1016/bs.ache.2022.03.001⟩.

Meuwly, F., von Stockar, U., Kadouri, A., 2004. Optimization of the medium perfusion rate in a packed-bed bioreactor charged with CHO cells. Cytotechnology 46 (1), 37–47. https://doi.org/10.1007/s10616-005-2105-z.

Moumné, L., Marie, A.-C., Crouvezier, N., 2022. Oligonucleotide therapeutics: from discovery and development to patentability. Pharmaceutics 14 (2), 260. https://doi.org/10.3390/pharmaceutics14020260.

Narayanan, H., Sponchioni, M., Morbidelli, M., 2022. Integration and digitalization in the manufacturing of therapeutic proteins. Chem. Eng. Sci. 248, 117159 https://doi.org/10.1016/j.ces.2021.117159.

Nienow, A.W., 2021. The Impact of Fluid Dynamic Stress in Stirred Bioreactors – The Scale of the Biological Entity: A Personal View. Chem. Ing. Tech. 93 (1–2), 17–30. https://doi.org/10.1002/cite.202000176.

Paredes, E., Aduda, V., Ackley, K.L., Cramer, H., 2017. Manufacturing of Oligonucleotides. In: Comprehensive Medicinal Chemistry III. Elsevier, pp. 233–279. https://doi.org/10.1016/B978-0-12-409547-2.12423-0.

Pereira, P., et al., 2016. Advances in time course extracellular production of human pre-miR-29b from Rhodovulum sulfidophilum. Appl. Microbiol Biotechnol. 100 (8), 3723–3734. https://doi.org/10.1007/s00253-016-7350-x.

Pereira, P., Queiroz, J.A., Figueiras, A., Sousa, F., 2017. Current progress on microRNAs-based therapeutics in neurodegenerative diseases. WIREs RNA 8 (3). https://doi.org/10.1002/wrna.1409.

Ponchon, L., Beauvais, G., Nonin-Lecomte, S., Dardel, F., 2009. A generic protocol for the expression and purification of recombinant RNA in Escherichia coli using a tRNA scaffold. Nat. Protoc. 4 (6), 947–959. https://doi.org/10.1038/nprot.2009.67.

Ponchon, L., Dardel, F., 2007. Recombinant RNA technology: the tRNA scaffold. Nat. Methods 4 (7), 571–576. https://doi.org/10.1038/nmeth1058.

Pörtner, R., 2015. Bioreact. Mamm. Cells 89–135. https://doi.org/10.1007/978-3-319-10320-4_4.

Shepherd, T.R., Du, R.R., Huang, H., Wamhoff, E.-C., Bathe, M., 2019. Bioproduction of pure, kilobase-scale single-stranded DNA. Sci. Rep. 9 (1), 6121. https://doi.org/10.1038/s41598-019-42665-1.

Smith, C.I.E., Zain, R., 2019. Therapeutic oligonucleotides: state of the art. Annu Rev. Pharm. Toxicol. 59 (1), 605–630. https://doi.org/10.1146/annurev-pharmtox-010818-021050.

Walther, J., et al., 2019. Perfusion cell culture decreases process and product heterogeneity in a head-to-head comparison with fed-batch. Biotechnol. J. 14 (2) https://doi.org/10.1002/biot.201700733.

Warikoo, V., et al., 2012. Integrated continuous production of recombinant therapeutic proteins. Biotechnol. Bioeng. 109 (12), 3018–3029. https://doi.org/10.1002/bit.24584.

Wolf, M.K.F., et al., 2019a. A two-step procedure for the design of perfusion bioreactors. Biochem Eng. J. 151, 107295 https://doi.org/10.1016/j.bej.2019.107295.

Wolf, M., Bielser, J.-M., Morbidelli, M., 2020. Perfusion Cell Culture Processes for Biopharmaceuticals. Cambridge University Press. https://doi.org/10.1017/9781108847209.

Wolf, M.K.F., Lorenz, V., Karst, D.J., Souquet, J., Broly, H., Morbidelli, M., 2018. Development of a shake tube-based scale-down model for perfusion cultures. Biotechnol. Bioeng. 115 (11), 2703–2713. https://doi.org/10.1002/bit.26804.

Wolf, M.K.F., Müller, A., Souquet, J., Broly, H., Morbidelli, M., 2019b. Process design and development of a mammalian cell perfusion culture in shake-tube and benchtop bioreactors. Biotechnol. Bioeng. 116 (8), 1973–1985. https://doi.org/10.1002/bit.26999.

Xiong, H., Veedu, R.N., Diermeier, S.D., 2021. Recent advances in oligonucleotide therapeutics in oncology. Int. J. Mol. Sci. 22 (7), 3295. https://doi.org/10.3390/ijms22073295.

Yamada, Y., 2021. Nucleic acid drugs—current status, issues, and expectations for exosomes. Cancers (Basel) 13 (19), 5002. https://doi.org/10.3390/cancers13195002.

Yang, J.-D., Angelillo, Y., Chaudhry, M., Goldenberg, C., Goldenberg, D.M., 2000. Achievement of high cell density and high antibody productivity by a controlled-fed perfusion bioreactor process. Biotechnol. Bioeng. 69 (1), 74–82. https://doi.org/10.1002/(SICI)1097-0290(20000705)69:1<74::AID-BIT9>3.0.CO;2-K.

Yu, A.-M., Jian, C., Yu, A.H., Tu, M.-J., 2019. RNA therapy: Are we using the right molecules? Pharmacol. Ther. 196, 91–104. https://doi.org/10.1016/j.pharmthera.2018.11.011.

Zhang, X., et al., 2009. Efficient oxygen transfer by surface aeration in shaken cylindrical containers for mammalian cell cultivation at volumetric scales up to 1000L. Biochem Eng. J. 45 (1), 41–47. https://doi.org/10.1016/j.bej.2009.02.003.